EVALUATING FEMTOSECOND LASER ABLATION OF GRAPHENE ON SiO_2/Si SUBSTRATE

Paper M602

Tianqi Dong[1], Martin Sparkes[1], Colm Durkan[2], William O'Neill[1]

[1] Institute for Manufacturing, University of Cambridge, Cambridge, CB3 0FS, United Kingdom
[2] The Nanoscience Centre, University of Cambridge, Cambridge, CB3 0FF, United Kingdom

Abstract

We demonstrate a uniform single layer micro-pattern of graphene on 300 nm thick SiO_2 on a Si substrate using a 1030 nm, 280 fs laser. The cutting process was conducted in air, the pattern defined through the motion of a high-precision translation stage. Approximately 1.6 μm wide graphene micro-channels were cut with uniform widths and well defined edges. The ablation threshold of graphene was determined to be 66 ~ 120 mJ/cm^2, at which the selective removal of graphene was achieved without damage to the SiO_2/Si substrate. SEM images revealed high quality cuts (standard deviation 40 nm) with little damage or re-deposition. Raman maps showed no discernible laser induced damage in the graphene within the ablation zone. Atomic force microscopy (AFM) revealed an edge step height ranging from less than 2 nm to 10 nm, suggesting little removal of SiO_2 and no damage to the silicon (the central path showed sub ablation threshold swelling). The effect of the ultrafast laser on the surface potential at the cut edge has been measured and it showed a distinguishable boundary.

Introduction

Graphene, a form of carbon where the atoms are arranged in a honeycomb lattice, offers extremely high carrier mobility, mechanical flexibility and optical transparency. It has attracted enormous interest, emerging as an exciting new material with the potential to impact many areas of fundamental research and high-performance devices [1-3]. It is a challenge to manufacture graphene with nano/micro size features for devices such as FET transistors [4] or tuneable tetrahertz plasmonic resonators [5]. Lithographic methods can be used to achieve precisely located nano/micro patterning and cutting on graphene; various techniques exist e.g. helium ion microscope lithography [6], resist-free soft lithography [7] and block co-polymer lithography [8]. These involve a long sequence of process operations, which may also increase the risk of polymeric contamination. Femtosecond laser micromachining has the advantages of limited thermal effects, high processing speed [9] and capability to machine complex shapes. Current studies have shown its potential in direct cutting and patterning, offering free-form post-patterning of general graphene devices. Roberts *et al* demonstrated a clean micro-hole by using a single short laser pulse, 50 fs, with a wavelength of 790 nm [10] and Zhang *et al* obtained 25 μm wide channels of graphene on glass substrate by using 100 fs Ti: sapphire laser with a central wavelength of 800 nm [11]. More recently, Sahin *et al* used a 550 fs laser with a wavelength of 343 nm to achieve a 400 nm wide ablation channel on SiO_2/Si substrates. By controlling the pulse energy and speed value, cut samples without damaging the Si substrate were achieved, however, the graphene was not completely removed [12].

This study looks to optimise the pattern precision of the patterned graphene and understand the substrate damage and as hence provide information on maximising performance and reliability [13] leading toward device manufacturing. In this paper, we present 280 fs laser direct patterning on single layer graphene on SiO_2/Si substrate with a 300 nm SiO_2 layer. The damage threshold of graphene was found to be 66 ~ 120 mJ/cm^2.The peak fluence was lower than the damage fluence of silicon [14], preventing Si ablation. Optimum cut quality was achieved under the following conditions: 23.4 nJ, a traverse speed of 1.5 mm/s and focal spot diameter of 4.16 μm modulated at 5 kHz.

Theory

The challenge of using a femtosecond laser to fabricate a graphene device on SiO_2/Si substrate is to avoid damaging the Si substrate, which is critical due to its low ablation threshold. Graphene can only absorb 2.3 % of light (300 nm < λ< 1100 nm) [15] and the SiO_2 layer is almost transparent at the same range [16]. At a wavelength of 1030 nm, the laser light penetrates into the Si with an absorption depth of around 300 µm [17]. The damage threshold of Si is reported to be around 340 mJ/cm^2, which is higher than that of Si at 343 nm (100 mJ/cm^2). This range of thresholds offers the potential to achieve complete removal graphene without causing damage the substrate.

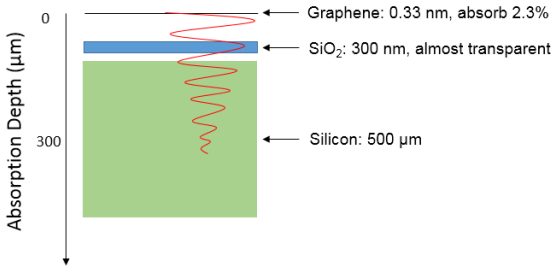

Fig. 1 Schematic of light absorption of graphene on SiO_2/Si substrate at 1030 nm.

Femtosecond laser processing offers high peak intensity. During the ablation process, the bonds in graphene and SiO_2 may break down and reform new bonds between Si and C on the surface of the substrate, bond energy shown in Table 1.

Table 1. Average bond energies.

Bond	Average bond energy (kJ/mol)	Reference
Carbon bond in graphene	480 ~580	[18]
SiO_2	408	[19]
Si-C	360	[20]

Experiment Setup

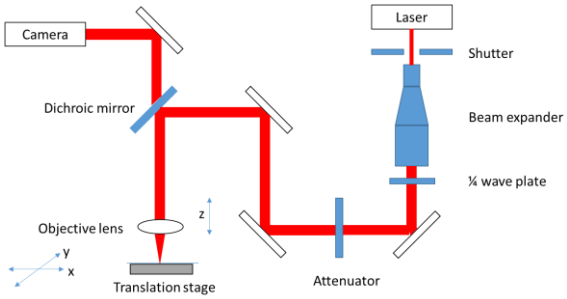

Fig. 2 Experimental setup of femtosecond laser machining system.

Fig.2 illustrates the experimental setup. The monolayer graphene used in this process was grown by chemical vapour deposition (CVD) on a 25 µm copper foil. It was then transferred onto a SiO_2/Si substrate as described in [21]. The pulse duration was measured with an optical autocorrelator (APE PulseCheck USB). Laser processing was carried out at room temperature in air with parameters listed in Table 2. The cutting path was controlled through the motion of a high-precision translation stage. The laser power was fine-tuned with a diffractive attenuator. The laser beams were circularly polarised and focused by an NA=0.35 objective lens (12 OI 09, Comar Optics) with a focal length of 12.7 mm to a spot diameter of 4.16 µm.

Table 2. Laser parameters.

Laser model	Amplitude Systèmes Satsuma
Wavelength	1030 nm
Duration	280 fs
Beam radius	2.2 mm
M^2	1.1

Results and discussion

Laser ablation

Ten groups of lines were cut with sample traverse speeds ranging from 0.05 to 3 mm/s with pulse energies of 23.4 nJ, 12.1 nJ and 5.90 nJ. However, the lines processed with 5.90 nJ showed no evidence of cutting by observation from both optical microscope and SEM (Zeiss 1540XB Crossbeam). With pulse energy of 23.4 nJ at speed of 0.05 mm/s, the Si substrate was

damaged. For the same pulse energy, the kerf width decreased as the cutting speeds increased, Fig. 3. Both of the variations showed cutting speeds around 1.5mm/s with the lowest standard error. For a pulse energy of 12.1 nJ, the optimum window of cutting, which was defined as the lowest standard deviation of the kerf width measurement, was found to be 1.0 ~ 2.0 mm/s. For 23.4 nJ, the optimum window was larger, ranging from 0.5 mm/s to 3.5 mm/s. The waviness in the kerf edge is attributed to slight variations of both the coating and laser giving pulse to pulse variation in diameter.

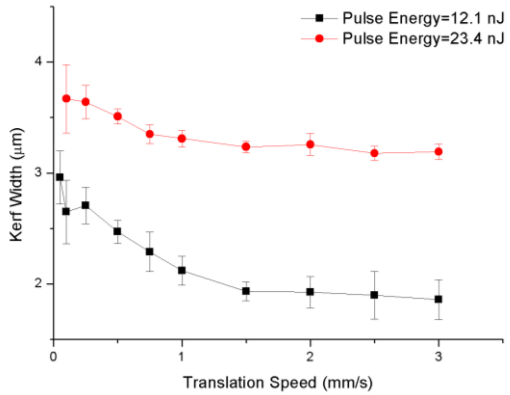

Fig. 3 Variation of kerf width with cutting speed for difference pulse energies.

The cutting quality can be observed through SEM images. Fig. 4 gives detailed information on the edge quality of a uniform cutting channel with width of 3.24 ± 0.04 μm.

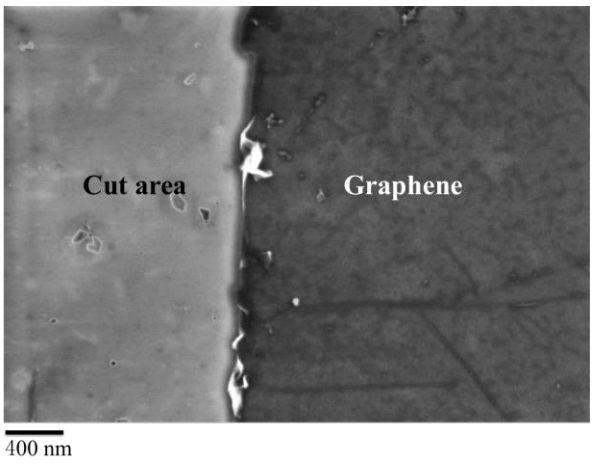

Fig. 4 SEM image of a cut processed with 1.5 mm/s, 23.4 nJ.

The damage threshold of graphene can be calculated via the following equation [22]:

$$F_{th} = \frac{2E_p}{\pi\omega_0^2}\exp(-\frac{d^2}{2\omega_0^2})$$

where E_p stands for the pulse energy, ω_0 is the beam spot radius after the focusing lens and d is the ablation diameter. The laser processing window to ablate graphene was determined to be 66 mJ/cm^2 ~ 120 mJ/cm^2 at room temperature in air.

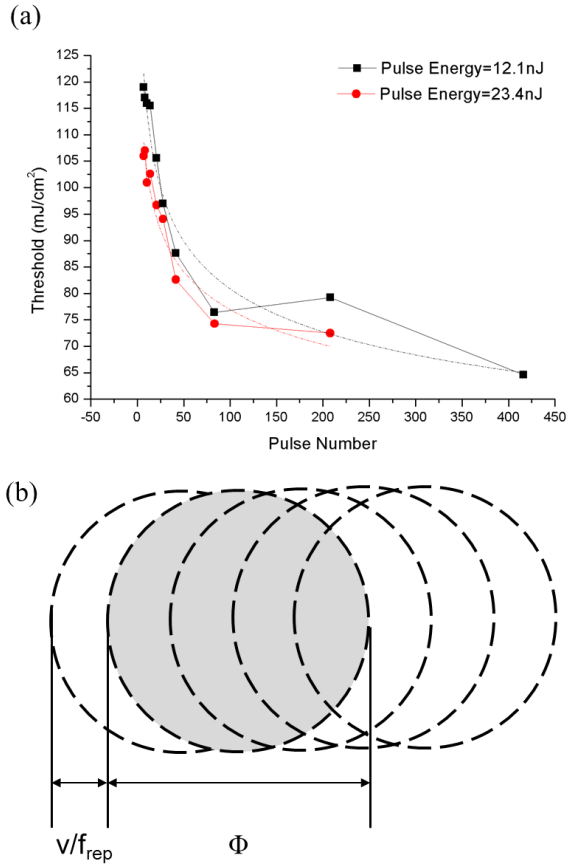

Fig. 5 Variation of damage threshold of graphene with pulse number or different pulse energies. The pulse number is estimated from the pulse overlap of a train of spot that moved at a constant speed.

Compared to reported thresholds, Table 3, the experimental results show lower values, down to 66 mJ/cm^2 (Fig. 5), this possibly can be explained by the incubation effect, which means the ablation threshold by femtosecond pulses is lowered as the pulse number

on the same area is increased. According to the cumulative equation [23]:

$$F_{th}(N) = F_{th}(1)N^{s-1}$$

Where $F_{th}(1)$ and $F_{th}(N)$ are the single-shot and N-shot damage thresholds, respectively. S is known as incubation coefficient which quantifies the degree of incubation behaviour. Assuming there is no incubation effect, the width of the patterning line would be always equal to the diameter of single-shot site, the estimation of pulse number was proposed in [23], which is expressed as $N = \frac{\Phi}{v/f_{rep}}$, where Φ is the spot size of focused laser beam, v represents processing speed and f_{rep} is pulse repetition rate.

For a pulse energy of 12.1 nJ, the single-shot damage threshold and incubation coefficient can be calculated to be 139 mJ/cm^2 and 0.87. For 23.4 nJ, the corresponding values are 163.3 mJ/cm^2 and 0.85. The calculated single-shot thresholds are in a good agreement with the literature, Table 3. Thus, the lower ablation thresholds ablation obtained (66 mJ/cm^2) could be qualitatively explained by the incubation effect.

Table 3. Reported damage threshold fluence of graphene, repetition rate 1 kHz.

Wavelength	**Pulse Duration**	**Threshold** (mJ/cm^2)	**Ref.**
790 nm	50 fs~1.6 ps	~200	[10]
800 nm	100 fs	160~210	[11]
800 nm	100 fs	89	[24]
343 nm	550 fs	~150	[15]

Atomic force microscopy

The benefit of a lower ablation threshold for graphene is avoiding damage to the Si substrate. As for a typical graphene FET device, an insulator (typically SiO_2) is used as capacitor between gate and body. To investigate the feasibility of using the femtosecond laser to pattern graphene FET devices, an analysis of any damage to the substrate is essential in order to optimise further fabrication steps.

To explore the dimensions and quality of the graphene sample post-ablation, atomic force microscopy (AFM) was used in tapping mode. As illustrated in Fig. 6 (a), the graphene rolls up at the edge (an example is in the dashed circle), also observed using SEM, Fig. 4. A representative line-section across the ablated region (along the light blue line in Fig. 6 (a)) is shown in Fig. 6 (b). The edge step height is around 6 nm, and there is no evidence of any removal of SiO_2 and no damage to the Si. With the kerf width measured to be 3.37 µm, the peak fluence is calculated as 261 mJ/cm^2, which is in the range between the melting and ablation thresholds of SiO_2 (Table 4).

Table 4. Ablation/melting threshold of substrate material at 1030 nm.

Material	**Threshold** (mJ/cm^2)		**Ref.**
100 nm thickness SiO_2	325±3 (Ablation)	233±4 (Melting)	[25]
Si	430		[11]

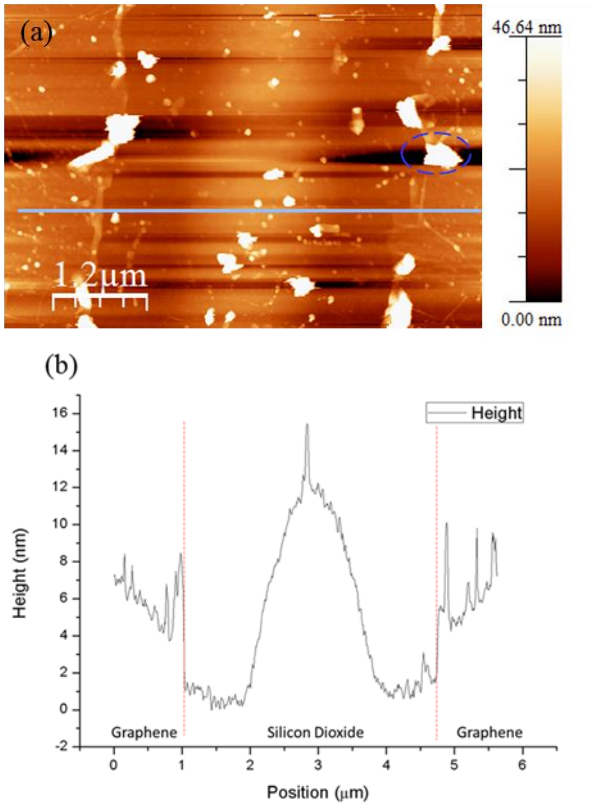

Fig. 6 (a) AFM topography image of a cut kerf with pulse energy of 17.8 nJ, processing speed 0.75mm/s. (b) Cross section map along the path shown by the horizontal line in (a).

The central region shows a sub-ablation threshold Gaussian-shaped swelling. The peak fluence (261 mJ/cm^2) is below the Si ablation threshold (~ 430 mJ/cm^2), however, due to the strong absorption of Si, such amount of energy could cause thermal expansion. As the fluence is above the silicon dioxide melting threshold, some expansion of Si could contribute to the apparent swelling of silicon dioxide.

Raman spectroscopy

The cut areas of ablated samples were examined by Raman spectroscopy, using 514 nm laser excitation with a 100x objective. The Raman laser spot size was around 0.7 µm. The laser power was lower than 1 mW to prevent the damaging of graphene [26]. G and D peaks, which lie at around 1560 cm^{-1} and 1360 cm^{-1} refer to the main features in the Raman spectra of carbon materials [27]. At ~ 2700 cm^{-1}, carbon materials also have a feature called the 2D peak. For graphene, this is particularly intense relative to the G peak [27].

Fig. 7 shows results from the uncut region, where intense G and 2D peaks occurred at around 1580 cm^{-1} and 2700 cm^{-1} on the unprocessed area. The G and 2D peaks, however, disappeared within the cut line. This proved that the laser completely removed the monolayer graphene on the Si substrate. Comparison to interpretation in cited literature are discussed in the next section.

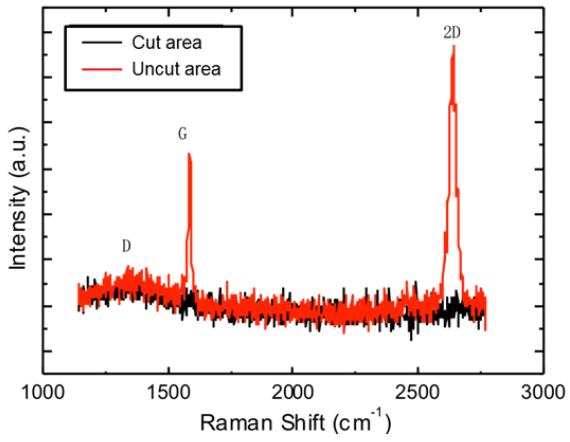

Fig. 7 Raman spectra of the cut base and uncut area

Since the edges break the translation symmetry of graphene, they can be treated as defects [27]. To characterize the microscopic edge modification, the edge of the ablated sample (processed with 0.75 mm/s, 17.8 nJ) were scanned with the Raman microscope. Fig. 8 (b) shows the Raman spectra obtained at four positions along y = -19 line of the optical image in Fig. 8 (a). At x=2, 4, 6 µm, the low intense disorder-induced D peak, at around 1350 cm^{-1}, show no discernible laser induced collateral damage near the cutting edge benefitting from the ultrafast laser pulses. On the edge (x=0 µm), we observe increase of defect-activated D and D' peak. The ratios of $I(D)/I(G)$ at x=0, 2, 4, 6 µm were calculated as 0.11, 0.069, 0.071, 0.079, respectively. The D peak could be caused by the edge itself. In the literature, oxidation was argued as a possible contribution to this D peak [11, 15, 28], however, the explanation requires further validation.

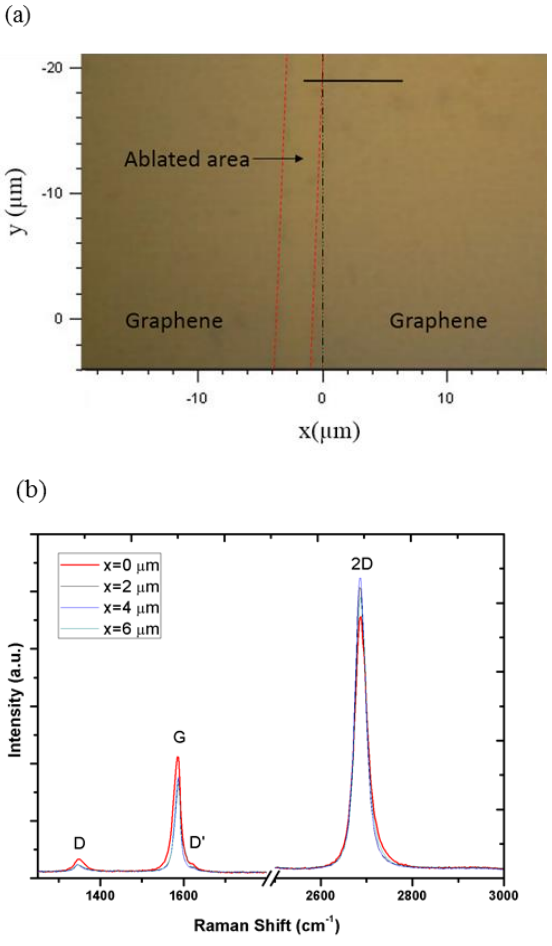

Fig. 8 Optical image of femtosecond pulse damage spot (a) and Raman spectra D, D', G and 2D peak (b) at four different locations, gradually away from the edge of laser ablation.

Kelvin Probe Force Microscopy

From the previous work, we know that both the Si substrate and graphene near the cutting edge were not damaged. The edge has shown a slight D peak increase and the SiO_2 experienced a Gaussian shape swelling. However, whether the femtosecond laser induced bond reformation on the SiO_2 surface as well as the modification of the cutting edge is unknown.

To further explore the cut region, AFM was used in Kelvin probe force mode. The experiments were carried out under ambient conditions, amplitude modulation measurement method selected. Kelvin probe force microscopy (KPFM) probes contact potential difference (CPD) between the conducting probe and the sample, providing quantitative mapping of the surface potential. Fig. 9 (a) shows the CPD image of the same cut kerf as shown in Fi.6 (a). It shows a clear and uniform potential difference ΔV_{CPD} between graphene and SiO_2, which was measured to be $\Delta V_{CPD} \approx 30\ mV$.

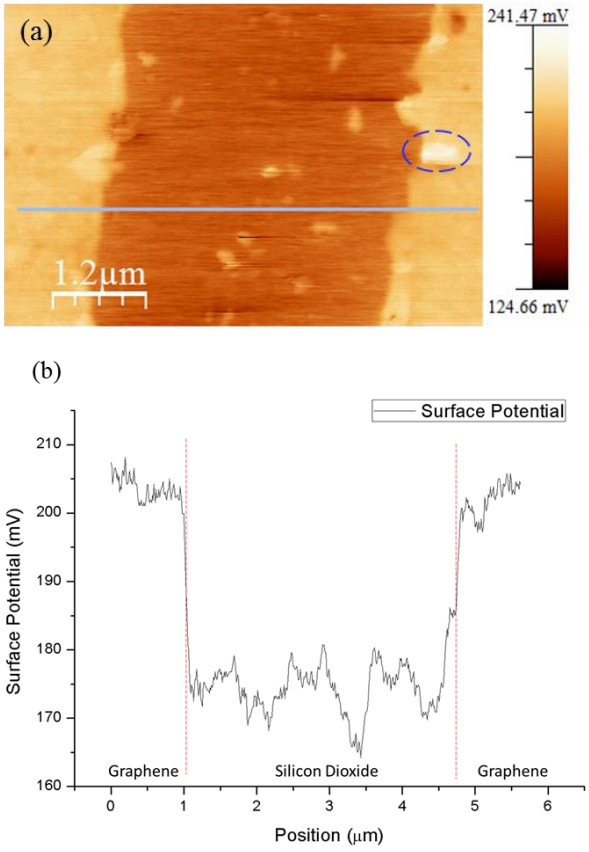

Fig 9. (a) Kelvin probe force microscopy (KPFM) surface potential map of the cut kerf shown in Fig. 6. A region at the edge where the graphene flake has folded over itself to create bilayer graphene is indicated by the dashed circle, having a higher CPD than the monolayer graphene (b) Cross section and surface potential maps along the path shown by blue horizontal line in (a).

The edges were distinguishable and showed a clear step in potential, with the surface potential as the rest of the graphene, which suggests no modification of other bonds. This supports that D peak generated at the edge of graphene was not due to the oxidation due to laser etching as explained in [11, 15, 28]. The folded flake of graphene at the edge, such as that shown in Fig. 6(a), showed a higher surface potential of around 40 mV. This is consistent with findings of others who show that the surface potential increases with the number of layers of graphene [29, 30]. On the SiO_2 region, the KPFM contrast is fairly uniform (~ 15 mV variation), implying no formation of SiC as a result of a chemical reaction between graphene and Si, since ΔV_{CPD} between graphene and SiC is around 100 mV [30]. These results indicate that during the femtosecond ablation process, there is no evidence of modification of SiO_2.

Conclusion

A 280 fs fibre laser has been evaluated for patterning of monolayer graphene on a SiO_2/Si substrate. We have demonstrated an effective technique for direct laser profiling of single layer graphene on this substrate.

1. The optimum channel was produced with a speed of 1.5 mm/s and a pulse energy of 23.4 nJ (pulse number ~13.8). The width was measured to be 3.24 ± 0.04 μm.

2. The ablation threshold was determined to be in the range of 66 mJ/cm^2 ~ 120 mJ/cm^2. It is lower than the values reported in the literature which could be explained by incubation effects.

3. With these parameters only graphene was removed, giving negligible substrate damage due to the lower ablation threshold of graphene relative to SiO_2 and Si.

4. Swelling was evident when graphene had been removed as a result of below threshold interaction of the laser and Si substrate.

5. The increased D peak in proximity of the machined channel was attributed to graphene edges, rather than oxidation as a result of laser processing. The edges can

be treated as defects as they break the translation symmetry of graphene.

Acknowledgement

This work was supported by The Engineering and Physical Sciences Research Council (EPSRC) and National University of Defence Technology (NUDT). The authors also thank Cambridge Graphene Centre (CGC).

References

[1] Novoselov, K.S. , Geim, A.K. , Morozov, S.V. , Jiang, D., Zhang, Y. , Dubonos, S.V., Grigorieva, I.V., Firsov, A.A. (2004) Electric Field Effect in Atomically Thin Carbon Films, Science 306, 666.

[2] Geim, A.K., Novoselov, K. S. (2007) The rise of grpahene, Nature Material, 6(3), 183-191

[3] Bonaccorso, F., Sun,Z., Hasan, T., Ferrari A.C. (2010) Graphene photonics and optpelectronics, Nature Photonics 4 (9), 611-622

[4] Schwierz, F. (2010) Graphene transistors, Nature Nanotechnology, 5, 487-496

[5] Ju, L., Geng, B., Horng, J., Girit, C., Martin,M., Hao, Z., Bechtel, H. A., Liang, X., Zettl, A., Shen, Y.R.&Wang.F. (2011) Graphene plasmonics for tunable terahertz metamaterials. Nature Nanotechnology. 6, 630–634.

[6] Bell, D.C., Lemme, M.C., Stern, L.A., Williams, J.R.&Marcus, C.M.(2009) Precision cutting and patterning of graphene with helium ions, Nanotechonology, 20 455302(5pp)

[7] George, A., Matthews, S., Gastel, R.V., Nijland, M., Gopinathan, K., Brinks, P., Venkatesa, T.& Elshof, J. E.(2012) Large area resist-free soft lithographic patterning of graphene, Small 9(5), 711-715.

[8] Choia,D., Kurua, C ., Choiab,C., Noha, K., Hongc, S.K., Dasd, S., Choid, W. & Jinab, S.(2014) Nanopatterned graphene field effect transistor fabricated using block co-polymer lithography, Materials Research Letters 2(3) 131-139

[9] Rizvi, N.H (2003) Femtosecond laser micromachining: current status and applications, RIKEN Review. 50, 107.

[10] Roberts, A., Cormode, D., Reynolds, C. Newhouse-Illige,T., LeRoy,B. J., Sandhu, A.S.(2011) Response of graphene to femtosecond high-intensity laser irradiation, Applied Physics Letter 99, 051912

[11] Zhang, W., Li, L., Wang, Z.B., Pena, A.A., Whitehead, D.J., Zhong, M.L., Lin, Z.& Zhu, H.W. (2012) Ti:sapphire femtosecond laser direct micro-cutting and profiling of graphene, Applied Physics A.109, 291-297

[12] Sahin, R., Simsek, E.&Akturk, S.(2014) Nanosclae patterning of graphene through femtosecond laser ablation, Applied Physics Letters 104, 053118

[13] Lee, J.H., Balasubramanian, K., Weitz., R.T., Burghard, M.& Kern, K.(2008) Contact and edge effects in graphene device. Nature nanotechnology 3, 486

[14] Thorstensen, J., Foss, S.E. (2012) Temperature dependent ablation threshold in silicon using ultrashort laser pulse, Journal of Applied Physics, 112, 103514

[15] Kuzmenko, A. B., van Heumen, E., Carbone, F. & van der Marel, D. (2008), Universal Optical Conductance of Graphite, Phys. Rev. Lett. 100, 117401

[16] Kitamura, R., Pilon, L. & and Jonasz, M. (2007) Optical constants of silica glass from extreme ultraviolet to far infrared at near room temperature, Applied Optics, 46, 33.

[17] http://www.pveducation.org/pvcdrom/materials/optical-properties-of-silicon .

[18] Feng, J., Li, W., Qian, X., Qi, J., Qi, L. &Li, J. (2012) Patterning of graphene, Nanoscale, 4 (16) , 4883–4899.

[19] https://www.electrochem.org/dl/ma/203/pdfs/2026.pdf

[20] http://butane.chem.uiuc.edu/cyerkes/Chem104ACSpring2009/Genchemref/bondenergies.html, Referenced from Chemistry by Zumdahl (5th ed.) Table 8.4 on page 373.

[21] Bonaccorso, F., Lombardo, A., Hasan, T., Sun, Z., Colombo, L.&Ferrari, A. C.(2012) Production and processing of graphene and 2d crystals, Material Today, 15, 564

[22] Zheng, B., Jiang, G., Wang, W., Wang, K. & Mei,.X (2014) Ablation experiment and threshold calculation of titanium alloy irradiated by ultra-fast pulse laser, AIP advances 4, 031310

[23] Xiao, S., Gurevich, E.L.& Ostendorf, A. (2012), Incubation effect and its influence on laser patterning of ITO thin film, Applied Physics A 107, 333-338

[24] Yoo, J. H., I, J. B., Park, J. B., Jeon, H.& Grigoropoulos, C. P. (2012), Graphene folds by femtosecond laser ablation, Applied Physics Letters, 100, 233124

[25] Rublack, T. & Seifert, G. (2011) Femtosecond laser delamination of thin transparent layers from semiconducting substrate (Invited), Optical Material Express, 1(4), 543-550

[26] Passoni, M., Russo, V. , Dellasega, D., Causa, F., Ghezzi, F. , Wolversond, D. &Bottania, C. E. (2011) Raman spectroscopy of nonstacked graphene flakes produced by plasma microjet deposition, Journal of Raman Spectroscopy, 43 (7), 884-888

[27] Ferrari, A. C., (2007) Raman spectroscopy of graphene and graphite: Disorder, electron-phonon coupling, doping and nonadiabatic effects. Solid State Communications, 143 (1-2), 47-57

[28] Kalita, G., Qi, L., Namba, Y., Wakita, K.& Umeno, M (2011) Femtosecond laser induced micropatterning of graphene film, Materials Letters, 65 (11), 1569-1572

[29] Ziegler, D. , Gava, P., Güttinger, J. , Molitor, F. , Wirtz, L. , Lazzeri, M. Saitta, A. M. Stemmer, A. , Mauri, F. &Stampfer, C. (2011), Variations in the work function of doped single- and few-layer graphene assessed by Kelvin probe force microscopy and density functional theory, Phys. Rev. B 83, 235434.

[30] Panchal, V., Pearce, R., Yakimova, R. Tzalenchuk, A & Kazakova, O.(2013), Standardization of surface potential measurements of graphene domains, Scentific Reports, 3 2597.

Meet the Authors

Tianqi Dong graduated in 2010 from National University of Defence Technology with a BEng in Optoelectronic and Mphil in physic at University of Bath. After that she joint Institute for Manufacturing, University of Cambridge to pursue a PhD degree in Feb. 2014. The PhD project will investigate using ultrafast laser in graphene-based device and patterning graphene as a manufacturing step.

Martin Sparkes is a Senior Research Associate within the Institute for Manufacturing, University of Cambridge. He works within the Centre for Industrial Photonics principally as part of the EPSRC Centre for Innovative manufacturing in Ultra Precision. Research interests are currently focussed on ultra-precision laser based manufacturing processes.

Colm Durkan is a Reader in Nanoscale Engineering at the University of Cambridge. He obtained his degree and PhD in Physics from Trinity College Dublin during which time he designed and constructed the first scanning near-field optical microscope (SNOM) in the country, and made significant advances in our understanding of the mechanisms behind image formation in such systems. He then spent a year in Konstanz, Germany working in collaboration with ZEISS on the construction of a commercial microscope system.

William O'Neill is a Professor of Laser Engineering in University of Cambridge and Director of the Centre of Industrial Photonics, Institute for Manufacturing. He has wide ranging interests in areas related to laser based manufacturing.